Advances in Engineering Software 206 (2025) 103921

Contents lists available at ScienceDirect

Advances in Engineering Software

journal homepage: www.elsevier.com/locate/advengsoft

Research paper

Topology optimization of steel slotted dampers with the hybrid cellular automata technique

Angie Mendoza-Cuy [a], Oscar Begambre-Carrillo [a], Jesús D. Villalba-Morales [b,*]

[a] Escuela de Ingeniería Civil, Universidad Industrial de Santandaer, Carrera 27 Calle 9, Bucaramanga, Colombia
[b] Facultad de Ingeniería, Pontificia Universidad Javeriana, Av. 7 No 40-62, Bogotá, Colombia

ARTICLE INFO

Keywords:
Steel slotted dampers
Topology optimization
Cellular automatas
Metallic yielding dampers

ABSTRACT

Cellular automata is a computational technique that has proven valuable for solving engineering problems. In the field of structural optimization, it has been applied to find the optimal topology of a structure, given the similarities between the problem characteristics and the computational representation. This paper proposes a cellular automata-based methodology for the topology optimization of steel slotted dampers. A multi-objective approach is formulated to maximize the energy dissipation capacity and minimize the damper's mass. A single-cycle displacement protocol is utilized to determine energy dissipation capacity in Ansys. The results demonstrate that the proposed algorithm improves the optimal shape obtained from a configuration with vertical slots more efficiently than other two algorithms in the literature. The energy dissipation capacity was increased by 3.5 times while using only fourteen iterations to converge. By testing several initial slot configurations, the CA-based method proved to be less dependent on the initial decision. Finally, the effects of using a one-cycle displacement protocol, symmetry considerations, and the height/width ratio are also discussed.

1. Introduction

Today, computational intelligence (CI) techniques are widely used to solve everyday human problems. In civil engineering, CI has demonstrated its potential in a variety of problems, as evidenced by Demertzis et al. [1]. Despite that, the scientific community has yet to reach a consensus on defining CI. In this work, it is adopted Engelbrecht's definition [2], which relates CI to the development and use of computational paradigms that foster intelligence behavior to solve complex problems. From this perspective, Sumathi and Pannerselvam [3] classify CI techniques into computational paradigms such as artificial neural networks, fuzzy logic, evolutionary computation, swarm intelligence, and others. One of these paradigms is the cellular automata, a type of evolutionary computing. Cellular automata are mathematical idealizations of natural systems with discrete nature, so they may be viewed as simple construction parallel processing computers [4].

CI techniques have been applied to the seismic protection of structures to tackle different issues. Vaidyanathan [5] evaluated a multilayer perceptron neural network to predict the peak displacement, the effective period, and the effective damping of a three-story building with viscoelastic dampers. Abdulateef and Hejazi [6] used fuzzy logic to offer robustness in the vibration control of structures with magnetorheological dampers, addressing uncertainties associated with the loads and structural properties. Metaheuristics have been employed to optimize the configuration of structures equipped with seismic protection devices, as shown in Refs. [7–10]. Additionally, it is possible to determine the optimal shape of devices, such as Steel Slotted dampers [11–13]. The amount of energy that a SSP damper can dissip is related to the shape, size, number, and distribution of slots, as well as the thickness and dimensions of the plate. This complexity hinders the practical selection of the optimal shape for the plate, but there is no consensus on how is the best approach for solving the problem. One critical issue corresponds to the computational cost of calculating the energy dissipation capacity from the non-linear finite element analysis. To the authors' best knowledge, cellular automata have not been explored for problems involving SSP dampers.

More research is needed on applying cellular automata in civil engineering to understanding their capabilities. Qiao et al. [14] used a 3D cellular automata in the prediction of the effects of corrosion in reinforced concrete structures. Schadschneider [15] used cellular automata to model the traffic on a highway, considering that a maximum of one car can fill each cell. Su et al. [16] studied the problem

* Corresponding author.
E-mail addresses: angie2198580@correo.uis.edu.co (A. Mendoza-Cuy), ojbegam@uis.edu.co (O. Begambre-Carrillo), jesus.villalba@javeriana.edu.co (J.D. Villalba-Morales).

https://doi.org/10.1016/j.advengsoft.2025.103921
Received 4 October 2024; Received in revised form 23 February 2025; Accepted 29 March 2025
Available online 17 April 2025

of a piping breach in an earth-rock dam based on a representation of cellular automata and a transformation rule during the failure process of the soil dam. Ozelim and Cavalcante [17] employed a tridimensional array of cellular automata for modeling the pore network in soils. Feng et al. [18] modeled the surface runoff in an urban environment during rainfall, considering both the spatial and temporal domains. Araghi and Stouff [19] integrated cellular automata to define the layout of a set of residential buildings, considering the cells as specific installations. An exciting application of cellular automata is the topology optimization of structures due to the straightforward link between the problem representation and automata arrays. Tovar [20] used cellular automata combined with finite element modeling to obtain the optimal topology for 2D structures. From this experience, cellular automata are a feasible technique for determining the optimal shape of an SSP damper. In addition, cellular automata could be applied to other structural topological problems, including the definition of the topology of steel beams [21,22].

This research proposes a cellular automata approach to numerically optimize the topology of a steel slotted damper (SSD) from a predefined shape. Quality criteria are related to maximizing the energy dissipation capacity (EDC) for a given material area. The software Ansys is used to generate the finite element model of a given SSP damper and compute the EDC. Matlab is used to implement the optimization algorithm and connect with Ansys. It is worth mentioning that this research was carried out entirely using a numerical approach, but experimental results [23] were used to calibrate the finite element model of a vertical damper. The main characteristics of the proposed algorithm are:

- The mathematical foundations lie in the theory of cellular automata, which is used for the first time to optimize SSD dampers. This choice of algorithm was made due to the similarities between the topology optimization representation and the geometric characteristics of the damper.
- It derives an optimal topology for the rectangular-boundary SSP damper, considering the impact of the initial solution's geometry. This approach addresses the challenge of defining the best initial configuration for the device.
- It requires few assessments of the finite element model, thereby reducing the computational cost of the optimization process. Such a strategy has paramount importance due to the computational cost of the non-linear dynamic analysis.

In addition, this research discusses topics that affect the EDC prediction of an SSD damper, including its behavior under various cyclic displacements, the impact of an initial asymmetric configuration and loading protocol, and the role of the height-to-width ratio.

2. Finite element modeling of a steel slotted damper in ansys

Initially, a brief description of how steel-slotted dampers (SSDs) work to protect a building against an earthquake is presented. This explanation is supported with visual resources to ease the understanding of the problem. Typically, an SSD damper is installed in the structure as schematized in Fig. 1, where the device is directly connected to the beam in the upper part and to rigid braces in the lower part. Fig. 2 shows several examples of steel plates with various slot types and thicknesses, indicating that it is possible a huge number of possibilities. The thickness of the plate is located perpendicular to the beam axis to introduce a uniform behavior in the plate, which is assumed to be in the plane. SSD dampers are easy to manufacture, being made entirely of steel, and their installation process is straightforward for the construction industry. Therefore, these devices could be used in earthquake-prone developing countries for seismic protection because of their potentially lower cost compared to other devices.

It is worth mentioning that it is necessary to have a fully experimental characterization of the device to determine their behavior under cyclic load. In that sense, Fig. 3 presents an example of a device test, where a horizontal actuator imposes a cyclic displacement on the top of the device while the base is fixed. The main action principle is the energy dissipation of the seismic input through yielding of steel material in the plate induced by shear displacement. To achieve this, the plate thickness should be oriented perpendicular to the beam axis and have a low height-to-width ratio. After an earthquake, if the SSD is damaged, it requires a replacement. The behavior of the steel under cyclic loads has received significant attention from industry and academy, and an substantial number of devices has been proposed [24].

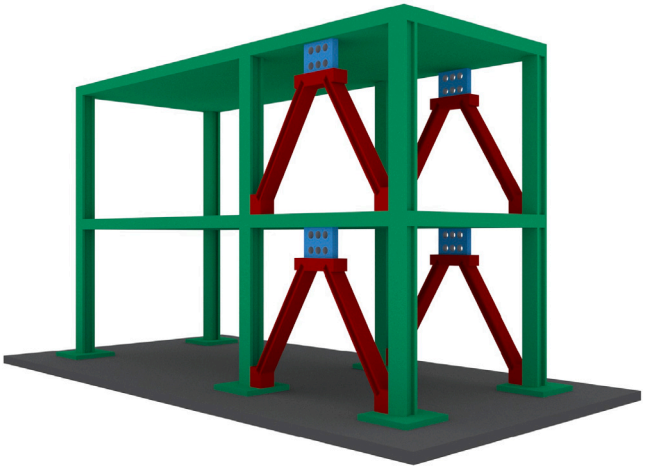

Fig. 1. SSD dampers installed on a Steel Frame.

Finite element (FE) modeling was performed using the APDL mode in the ANSYS software. This mode was selected to ease integration with the MATLAB computational routine that was developed for optimization, as shown in [25]. Fig. 4 shows the general procedure for the calculation of the energy dissipation capacity (EDC) of an SSD damper from a non-linear analysis in ANSYS and a given cyclic displacement protocol. It is assumed that the plate is thin, made of a single type of steel and that the damper is fully supported on the bottom side. Additionally, the user must provide the geometrical description of the slots. As can be seen, the FE modeling presents specifications discussed in the following paragraphs. It is worth mentioning that Ansys has previously been used in [26–28] to optimize other metallic dampers.

The first concern presented in Fig. 4(a) is the geometric description of the SSD damper. The user must define all the plate dimensions (width, height, and thickness) and slot information (location, shape, number, and size). These plate dimensions are the result of EDC requirements for a specific building project. As shown in Fig. 2, there are various possibilities for the shapes, distribution and quantity of the slot on the plate. The selection of configurations affects how the plate yields under a cyclic displacement, but there is no consensus on the procedure to define the initial configuration. The horizontal plates connect the damper to the upper beam and the lower support. It is worth mentioning that more than one type of SSD damper could be required for the different stories of the building.

The stress–strain curve that describes the behavior of the material is necessary. SSD dampers are made of ductile steel, such as A-36. Steel with low yield points can also be used [29], depending on the market availability on the construction site. This paper used a kinematic hardening assumption to consider the cyclic nature of the behavior of the steel material. Fig. 4(b) shows the bilinear representation of steel, which can be included in Ansys software. Other works have also used isotropic hardening [23] or mixed models [27], selected based on the agreement with the experimental results. In addition, more advanced phenomenological models could be used to improve the numerical assessment of the SSD Damper, see Refs. [30,31]. As there

(a) Circular slots (b) Rectangular slots (c) Triangular slots

Fig. 2. Examples of SSD dampers. Imagined by Midjourney AI.

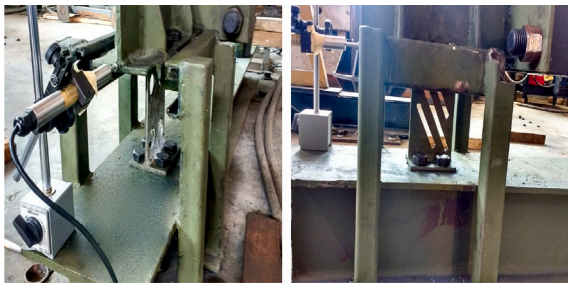

Fig. 3. Examples of an experimental test of the SSD dampers.

is no agreement on the best model, relying on experimental results for the calibration phase of the finite element modeling is recommended.

In the process of selecting the finite element type, two assumptions are defined concerning the SSD damper: (i) the plate is relatively thin, with a uniform behavior through the thickness and (ii) the main effect is due to shear stress, not considering possible movements out of the plane. Such approach was followed previously in other works such as [13,23,32]. From the Ansys element library, the Shell181 element (Fig. 4(c)) is a 3d quadrilateral plate type element with four nodes and six degrees of freedom. In this case, the option that forced the software to consider only translational degrees of freedom was activated: KEYOPTION(1) = 1. The Mindlin–Reissner theory is used to consider shear deformations. Other more robust elements have also been used in the literature, such as the 3D solid reported in [28]

As mentioned above, experimental testing of an SSD damper involves fixing the bottom part of the device and inducing horizontal displacement at the top. Fig. 4(d) illustrates the boundary condition defined for the model, where the entire bottom surface is fully restricted to translational movement, while the upper side is restricted only to vertical movement. These conditions simulate a relative horizontal movement between the extremes of the devices due to the difference between the movement of the upper beam and the top of the braces. The supporting braces transmit movement to the lower floor and are elastically designed to guarantee damper operation.

Despite the stochastic nature of earthquake movement, it is common practice to use a cyclic displacement protocol to assess the energy dissipation capacity of the device (see Fig. 4(e)). This protocol is imposed on the surface of the upper side of the SSD damper parallel to the beam axis. The protocol must be selected from the design code that rules on the construction site. Examples of such protocols include those defined by the documents ASCE 7-16 [33], FEMA-461 [34] and AISC [35] in the United States, as well as standards from Europe [36], China [37], and Japan [38]. The final configuration of the protocol depends on the project specifications for a specific type of damper.

Finally, it is necessary to integrate the numerical model of the device in step 4(f), as the size of the elements can influence the evaluation of the EDC. In Ansys, this process was implemented considering the default option. Table 1 shows the difference in the EDC for different element sizes for a plate. As expected, a convergence of the EDC for the lower element sizes is obtained. However, using these smaller element sizes increases the computational cost. A good trade-off between results precision and computation cost is achieved with a 2.5 mm size. For this size, the error is only 1% concerning the 1.0 mm size, but the computational time is reduced to 13%.

The Newton–Raphson method option in ANSYS solves nonlinear analysis in the time domain. The Line search option was activated, which improved the performance of finding the solution. Given the number of degrees of freedom in the FEM model of the damper, the Sparse Direct Solver was used for a more efficient algorithm. After the analysis, a post-processing stage is necessary to determine the Von-Misses stress state, the distribution of deformation energy, and the hysteresis cycles in the devices, as shown in Fig. 5. ANSYS directly computes the total deformation energy, which helps to assess the objective function during the optimization process.

3. Shape optimization of SSD dampers

Changing the shape of the slots on a steel plate is manufacture-friendly due to the simple configuration of the damper, as seen in Fig. 6. For the regular and basic slot configurations, it is possible to keep the same quantity of material, inducing a different energy distribution density for each configuration, as seen in Fig. 7. In addition, the height/width ratio affects the energy/mass ratio as the stress trajectories on the plates change during the cyclic movement. In that sense, it raises the question: ¿what will be the plate's shape that maximize the energy dissipation capacity during an earthquake movement?.

An optimization problem is configured to determine the optimal shape of the damper that maximizes its efficiency in dissipating seismic energy. Two types of computational problems are derived, depending on whether the amount of material can vary during the optimization process or not. Fig. 8 presents the case of the two types of optimization for an SSD damper with vertical slots. Fig. 8c shows that the material changed from the initial condition to an optimized shape. This is because the change in the mass could help to better exploit the energy dissipation. In 8b, the quantity of material is fixed. This condition obliges the algorithm to ensure that the quantity of material does not change between two consecutive iterations. It is worth mentioning that the user must define an initial configuration for the SSD damper in both cases. The symmetry concerning a vertical and horizontal axis through the plate's center point is generally considered to reduce the computational complexity of the problem. The final boundary of the plate significantly affects its overall behavior. Therefore, it is possible to use an interpolation function, such as B-Splines [39], to indicate how that transition should be.

In the FE model of the damper, each element in the mesh discretization is assigned a binary value: zero for a void and 1 for a material point. For SSD dampers, a rectangular domain for the plate is assumed, with the mesh size defining the number of positions to be specified. Fig.

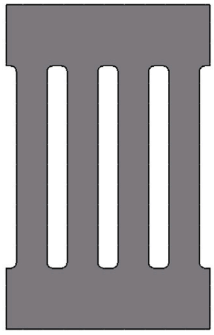

(a) Geometrical information

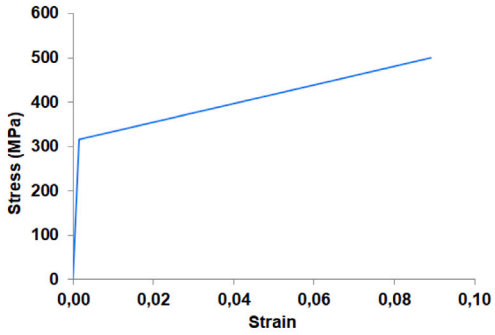

(b) Material

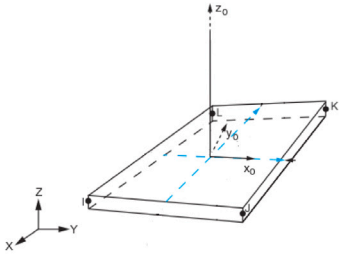

(c) Type of finite element

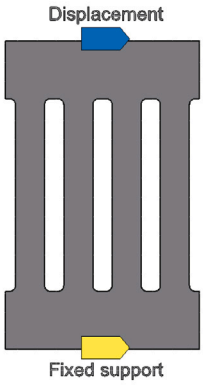

(d) Boundary conditions

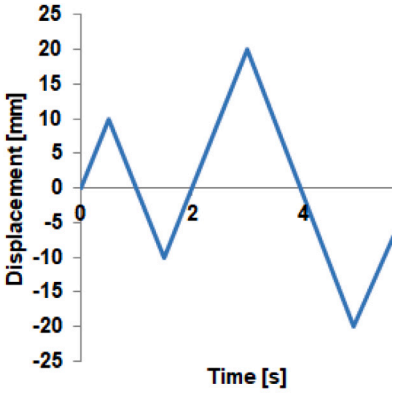

(e) Cyclic displacement protocol

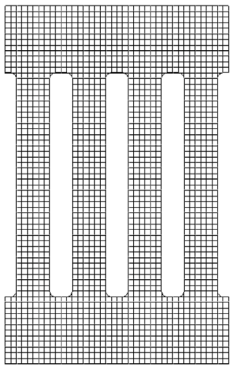

(f) Meshing

Fig. 4. Scheme of the finite element modeling of a SSD damper under a cyclic displacement protocol.

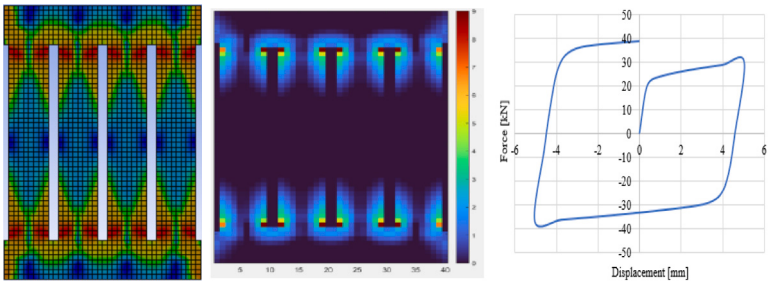

(a) Stress (b) Energy distribution (c) Hysteresis Cycle

Fig. 5. Example of post-processing.

Table 1
Impact of the mesh size on the computed deformation energy and the computational cost.

Mesh size (mm)	Deformation Energy (J)	Computation Time (min)	Difference (%)
1.0	1097	15.0	–
1.5	1100	7.0	0.27
2.5	1109	2.0	1.09
5.0	1125	0.5	2.05

Fig. 6. Examples of slotted damper.

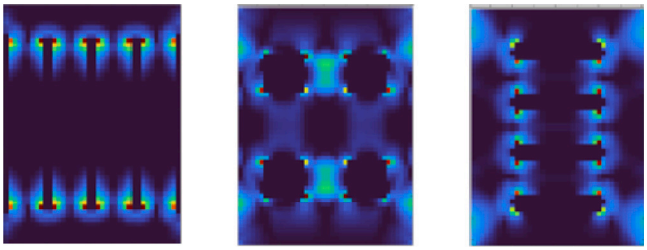

Fig. 7. Examples of energy distribution.

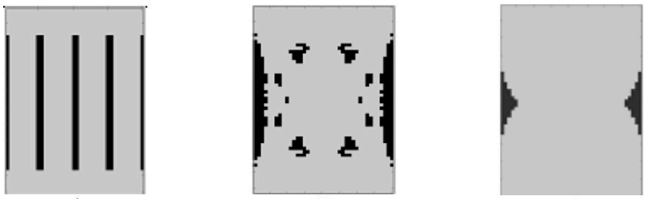

Fig. 8. Examples of energy distribution.

9 illustrates four computational representations, each corresponding to a different initial configuration of slots. As the topology changes during the iterative process, a strategy is needed to ease the finite element meshing. In this approach, voids are represented as material points with a very low modulus of elasticity. Therefore, the same mesh discretization is used in each iteration. The only constraint is that the elements must remain within the original boundary. Some studies use a one-cycle protocol [23] to determine the optimal shape [23] with the aim of reducing the computational cost associated with the optimization process. However, it is necessary to account for the effect of multiple cycles, as shown in [40].

Several metaheuristic and gradient-based approaches have been reported in the literature, which gives information on the optimal shape of a damper manufactured from a steel plate with slots. The gradient-based approach considers the computation of the derivatives of the energy dissipation function, as observed in [23,41]. In addition, it is possible to determine only the variation of the plate boundary, as presented in Ref. [40]. Metaheuristics approaches have been followed to ease the optimization process, highlighting algorithms such as Simulated Annealing [13] or Grey Wolf Optimizer [42]. The cost computational is critical when choosing the metaheuristic type, which is a disadvantage for a population-based metaheuristic. The majority of the optimal shapes obtained correspond to hourglass shapes for the slots [13,23]. An optimization algorithm could get stuck in a local optimum depending on the original configuration of the SSD damper, as shown in Ref. [13]. It is worth mentioning that there is no benchmark study to define the global solution for the SSD damper in a building, which implies further research.

4. Concept of celullar automatas in topology optimization

Cellular automata (CA) comprise a network of identical cells (slots) with an assigned state that can be represented in one or more dimensions. Each cell interacts with its defined neighbors and has a set of possible states, such as a black-and-white strategy. The state of each slot evolves by applying a set of local rules that consider the current state of the cells and those of its neighbors. It is worth mentioning that the application of the rule is carried out in parallel, accelerating the computations. This concept is illustrated in Fig. 10, where simple rules lead to the development of complex behavior in the popular game of life. That property of CA can be used to apply problems in different fields of knowledge such as spread of infectious diseases [43], management of evacuation from a sporting event [44], organizational management [45], music composition [46], understanding online public opinion [47] and protection of the Internet of Things [48]. Fig. 11 shows an example of a CA in nature, a typical distribution for a 3D structure, and a CA-based civil structure. The question now is how to use the CA technique to solve a given problem with specific characteristics. Detailed information on the conceptual and mathematical aspects of CA can be found in references such as [49,50].

There is a natural comparison between the CA 2D array in Fig. 10 and the optimization of the topology of a simply supported beam under a vertical load in the center. This is because the finite element mesh defined for a structure can be formulated in terms of voids and material points. Then, it is important to define a strategy for evolving the structure to its optimal shape. Hybrid CA [20] is an alternative for optimizing the mechanical topology of a solid structure by discretizing the physical domain into a regular array of CA. The state of the ith automaton is related to the presence or absence of material in the corresponding location, x, representing the CA mass. It also defines the state value corresponding to the stimulation of the CA. The state of the variables is assessed from the finite element analysis, which reduces the residual between external work and the internal energy to zero for each interaction. Each automaton locally modifies the design state variables until they reach the optimal value. This means that the rules aim to minimize the absolute error between the energy density of local deformation and the objective value. The algorithm begins with defining the design domain, the material properties, the load conditions, the boundary condition, and the initial values of the design variables. Then, the initial value of the state variables is computed using the finite element analysis of the structure. The evolution rule is applied to modify the design variable. Then, the convergence of the process is verified after no improvement is observed.

Fig. 12 presents an example of the application of the hybrid CA to a simply supported beam with a vertical load in the middle as proposed in [20] and which the authors implemented to assess its correct application. The method requires a posterior discretization

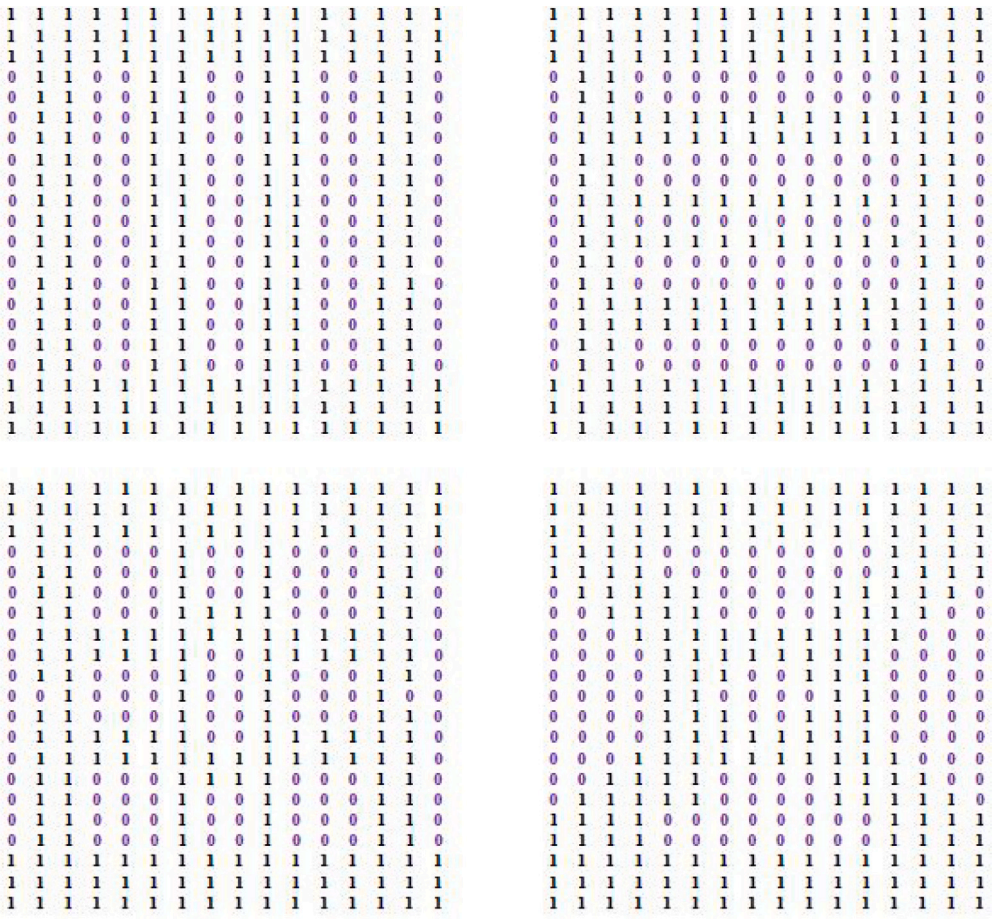

Fig. 9. Examples of computation representation for slotted dampers.

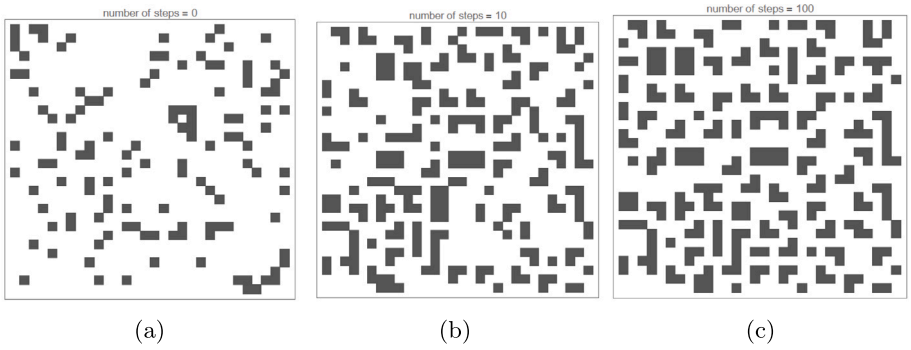

Fig. 10. Cellular automata for the game of life (https://demonstrations.wolfram.com/CellularAutomataWithModifiedGameOfLifeRules/). (a) 0 iterations, (b) 10 iterations and (c) 100 iterations.

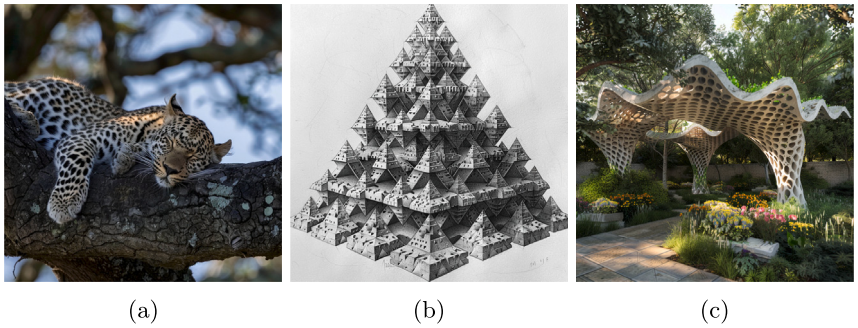

Fig. 11. Cellular automata as imagined by Midjourney IA for: (a) a leopard in nature, (b) 2d Typical distribution array and (c) a roof structure.

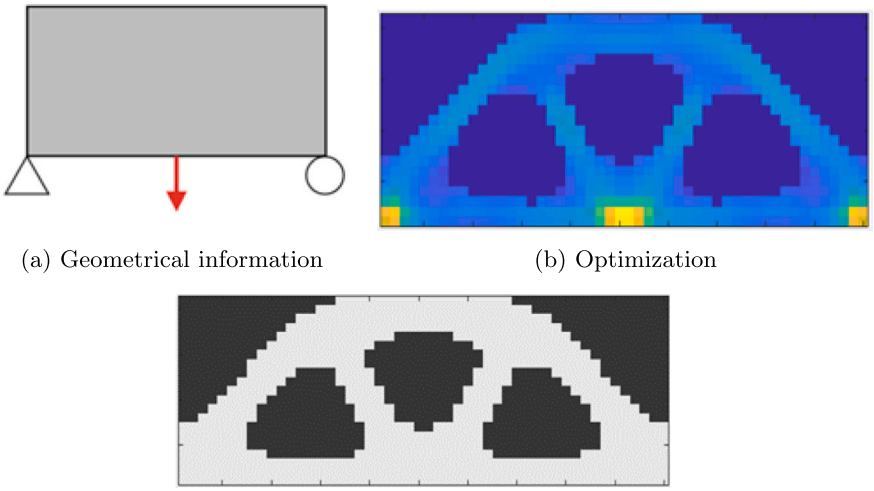

(a) Geometrical information (b) Optimization

(c) Discretization

Fig. 12. Example of optimization whit HCA - Michelle Beam.

process in Fig. 12(c) after the optimization process in Fig. 12(b). The HCA method is a computational technique that can obtain optimal topologies from local rules, even though the method is not an explicit optimization technique.

5. Application of cellular automatas in topology optimization of SSD

5.1. Formulation of the optimization problem

In this research, the Hybrid Cellular Automata Technique [20] is applied to determine the optimal shape of an SSD damper (see Fig. 6). As with any conventional optimization problem, it is necessary to establish a mathematical model that includes the objective function, the design variables, the design parameters, and the constraints. While defining the optimal SSD configuration, it is desired to reach two conflicting objectives: the maximization of deformation energy and the minimization of the mass of the SSD damper. It is used the following equation to transform the problem into a single-objective one:

$$\underset{x}{Min}\ c(x) = f(U) + g(M) \tag{1}$$

where $f(U)$ and $g(M)$ are functions of the deformation energy U and the mass of the damper M. x represents the domain of the problem, represented by the mesh of the finite element model. As the objectives are conflictive, Eq. (1) is transformed into:

$$\underset{x}{Min}\ c(x) = w \cdot \frac{U(x)}{U_0} + (1-w)\, g\frac{M(x)}{M_0} \tag{2}$$

where U_0 and M_0 are the initial values of the deformation energy and the mass, respectively. For a specific SSD damper configuration, such values are obtained from the finite element analysis in ANSYS, as presented in Section 2. w is a weight factor to consider the contribution of each term, ranging from 0 to 1. Since w is positive, the optimal solution is guaranteed to belong to the Pareto front.

The computational representation for the SSD damper is presented in Fig. 9, considering the possibility that the quantity of the mass varies during the optimization process. Thus, the design variables correspond to the possibility that each finite element in the rectangular domain has or does not have a material point. The design variables are binary type, where 0 indicates a void point and 1 indicates a material point. Thus, for the finite element located in the position (i,j) of the rectangular domain is given:

$$x_{(i,j)} = \begin{cases} 0 & \rightarrow void \\ 1 & \rightarrow material \end{cases} \qquad x_{(i,j)} \in \Omega_{SSD} \tag{3}$$

where Ω_{SSD} indicates the domain of the damper. The design parameters correspond to all the information that does not change during the evolutionary process. This includes the external dimension of the search space (width and height of the damper) and the steel properties (modulus of elasticity, density, hardening coefficient, ultimate strength). It also covers the cyclic displacement protocol, the supports and the parameters for finite element modeling. Finally, the problem does not present additional constraints.

5.2. Transforming an SSD configuration using heuristic rules

Cellular automata can be seen as a single solution-based optimization algorithm, since it transforms the current solution by applying mathematical operators. The transformation is based on the state variable, corresponding to the density of total energy deformation (the sum of the elastic and plastic deformation energy). Fig. 13 summarizes the procedure for turning a solution in the jth iteration into a new solution applying the following operations: (i) updating the target energy, (ii) updating the field variable, (iii) the updating of the design variable, and (iv) application of the local evolution rule.

The local rule of evolution presents the following structure:

$$x_i(t+1) = x_i(t) + \Delta x_i. \tag{4}$$

where i in the cell in the analysis and t is the current iteration. Δx_i is the change in mass and ranges from −0.1 to 0.1. This value depends on the error between the effective variable state $\bar{y}_i$ and the objective value $\bar{y}_i^*$. As defined by

$$\bar{e}(t) = \bar{S}_i(t) - \bar{y}_i^*(t) \tag{5}$$

The definition of the target deformation energy plays a very important role in balancing the mass fraction and dissipated energy. In this research, the average of the energy deformation for the entire domain was used as the objective variable, as follows:

$$y_i^* = \frac{\sum_{i=1}^{N} S_i}{N} \tag{6}$$

where N is the number of elements in the finite element model and S_i represents the deformation energy of the ith element.

The set of local evolution rules operates using the information from the neighborhood of each cell within the cellular automata array. The effective state variable $\bar{S}$ measures the average structural performance of a cell and its neighboring cells and the effective design variable $\bar{x}$ measures the average mass. This approach can be seen as a filtering

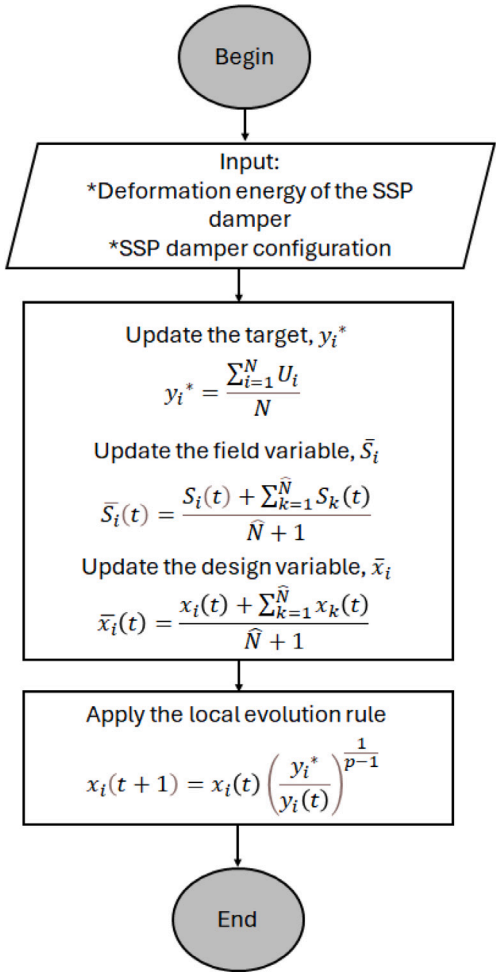

Fig. 13. Evolution rule.

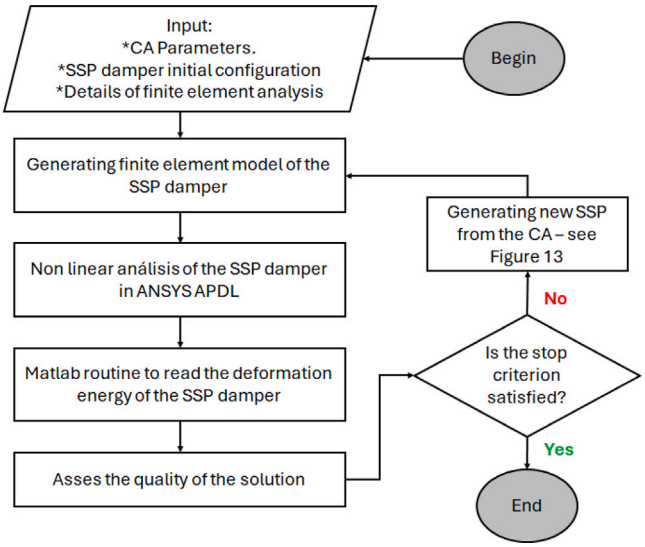

Fig. 14. Hysteresis Cycle for the initial and optimal configuration.

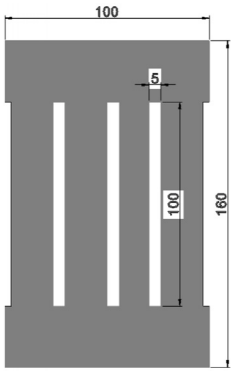

Fig. 15. Initial configuration device with vertical slots.

technique that reduces numerical instabilities, such as the chessboard or the mesh dependency. Then

$$\bar{S}_i(t) = \frac{S_i(t) + \sum_{k=1}^{\hat{N}} S_k(t)}{\hat{N}+1} \tag{7}$$

$$\bar{x}_i(t) = \frac{x_i(t) + \sum_{k=1}^{\hat{N}} x_k(t)}{\hat{N}+1} \tag{8}$$

where i and k correspond to the cell and the neighbors under analysis. t is the current iteration. $\hat{N}$ is the number of neighbor cells depending on the neighborhood type.

Although the HCA technique employs local rules to distribute material, the stop criterion for the iterative process relies on global information. To mitigate premature convergence, the convergence criteria in this study were based on mass changes between consecutive iterations. The mass change can be computed as

$$\Delta M(t) = \sum_{i=1}^{N} \left| x_i(t) - x_i(t-1) \right| \tag{9}$$

with the stop criterion given by:

$$\frac{\Delta M(t) + \Delta M(t-1)}{2} < 0.0001 \cdot N \tag{10}$$

5.3. General procedure and limitations

Fig. 14 presents the general procedure of the proposed CA for optimizing SSD dampers, considering the ANSYS software as a motor for finite element analyses. It is necessary that the user provides the entire information to configure the SSD damper, the description of the load protocol, the parameters of the finite element analysis and the parameters of the cellular automata. The stop criterion is defined as the stagnation of the deformation energy during three successive iterations. This method is equivalent to the one developed by Tovar [20], with application specific to the problem studied. It is worth mentioning that the proposed procedure does not require the computation of derivatives, easing the numerical procedure.

It is worth mentioning that the main limitations of the problem are related to:

- The behavior of the plate is limited to the plane of the device, where the main displacement occurs during the earthquake.
- The results are limited to considering the behavior for one loading cycle, which reduces the computation of the behavior of the device.
- The results depend on the ability of the material modeling to represent the behavior of the damper under cyclic load.
- The initial domain of the SSD damper is rectangular and is dependent on the height-width ratio.

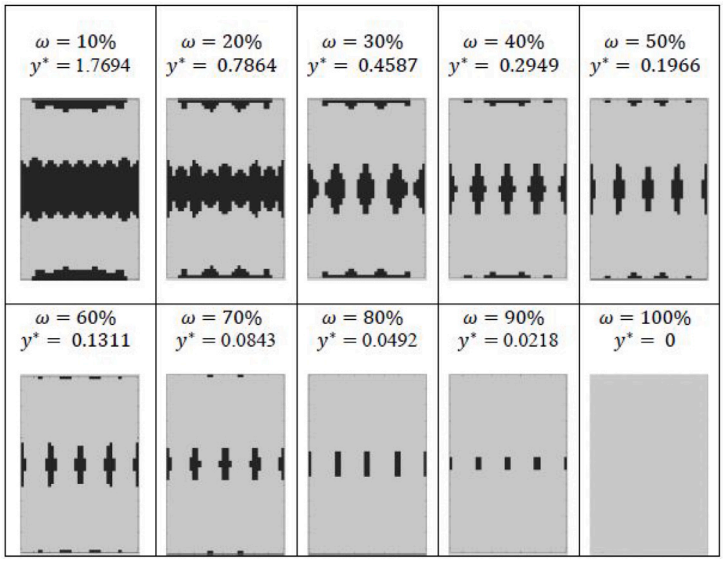

Fig. 16. Percentage of mass participation in the evolution rule for vertical slots.

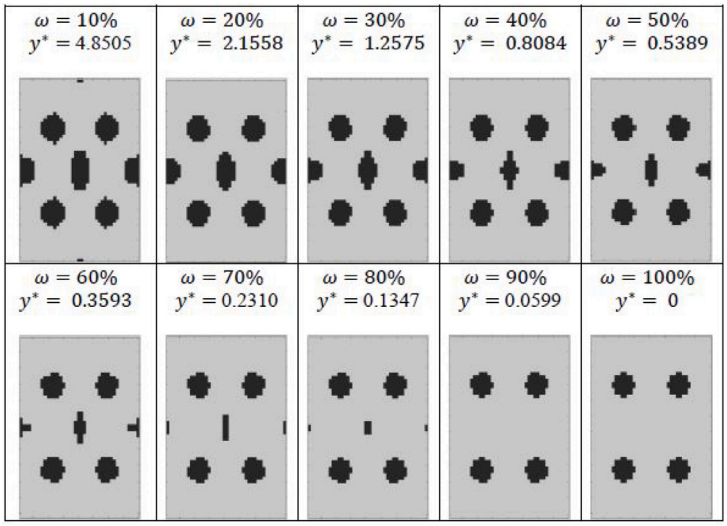

Fig. 17. Percentage of mass participation in the evolution rule for circular slots.

6. Numerical examples

6.1. Optimizing a SSD damper with vertical slots

In this investigation, the CA-based methodology was first tested for optimizing the topology of a configuration of an SSD damper with four vertical slots of 100 mm × 5 mm, as presented in Fig. 15. This configuration was chosen to compare the performance of the proposed methodology with the previous results obtained in Refs. [13,23]. All three numerical approaches use only one solution per iteration to solve the optimization problem. Such characteristic of this algorithm is essential for optimizing the shape of the SSD damper due to the computational cost of assessing the structural response by a non-linear finite element analysis. As mentioned in Section 5, there are three user-defined parameters to ensure the correct performance of the CA. These parameters correspond to the percentage of mass participation (w) for the calculation of the objective state variable in the evolution rule, the type of neighborhood, and the approximation factor.

Fig. 16 presents the impact of different values of w on the evolution of the cellular automata for a damper with vertical slots. The objective value $y*$ decreases as w increases, showing a critical range of values. For values lower than 20%, the mass participation is minuscule, which means that the dampers will not have enough material to maximize their EDC, and the probability of losing the physical sense of the plate increases, as observed in the two disconnected regions on the upper and lower part. Numerically, the generation of configurations with disconnected regions is possible due to the strategy of representing a void with a material that has a very low modulus of elasticity. It is worth mentioning that it is not physically possible to have disconnected regions in the SSD configuration. For values higher than 50%, it is noted that there are a high quantity of mass in the domain, which makes it difficult to remove material points to minimize the mass on the damper. Another case is presented using circles for the initial shape of slots, as shown in Fig. 17. In this case, values higher than 50% slightly change the topology of the damper, and this is because the initial geometry presented a high EDC value. No disconnected regions are observed for any of the w values. Taking into account the two above results, it was decided to use a w value of 30% for all the examples analyzed in this investigation.

Four cases were evaluated to determine the state and design variables, using all possible combinations of Moore and empty Neighborhoods. The first case involves assigning an empty neighborhood

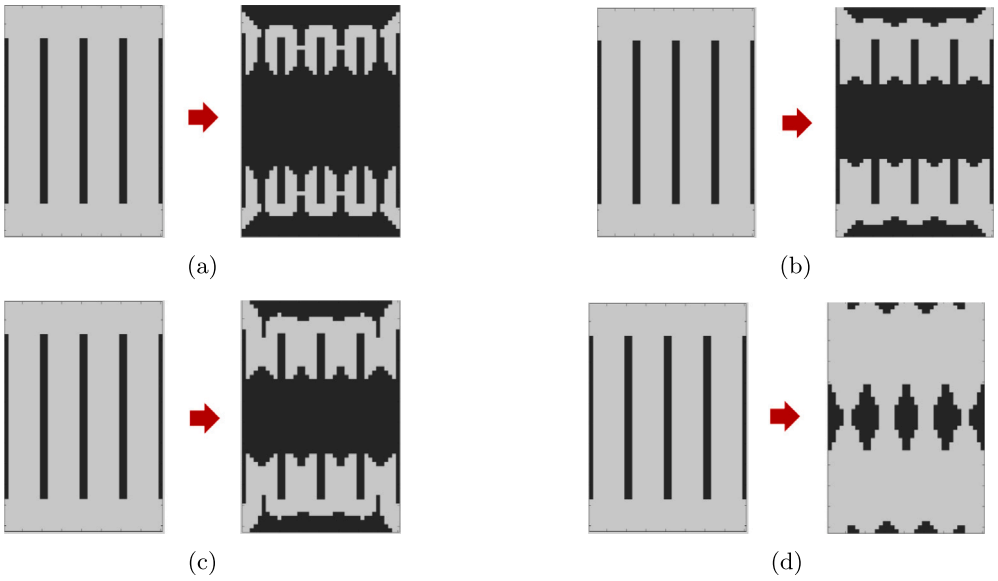

Fig. 18. Neighborhood size for the state and design variables: (a) E-E case, (b) M-E case, (c) E-M case and (d) M-M case.

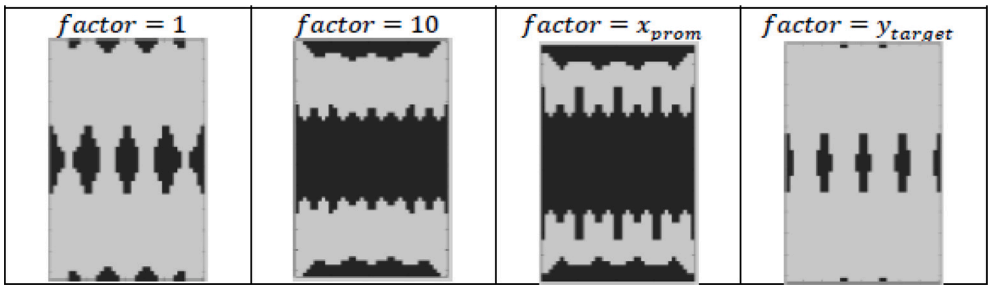

Fig. 19. Definition of the approximation Factor.

for the state and design variable (E-E case). In the second case, the state variable is modified to have a Moore neighborhood (M-E case). The third case does the opposite, assigning a Moore neighborhood to the design variable (E-M case). The four case uses a Moore neighborhood for both variables (M-M case). Fig. 18 shows the result for the first iteration in the SSD damper with vertical slots, showing the superiority of using the Moore neighborhood for both variables (M-M case). As can be seen, the other combinations of neighborhoods generate disconnected areas for the damper, compromising its physical representation. As happened for the damper in Fig. 16, it is necessary to avoid the situation of disconnected regions to have feasible dampers. In addition, it was observed that the transformation of void points into materials is numerically challenging for all cases. Therefore, the Moore neighborhood is used for the following analysis.

The final CA parameter to be defined is the approximation factor, which influences the connectivity of all the material points in the damper. The definition strategy involved observing the value of the design variable after applying the evolution rule. For the case of the SSD damper with vertical slots, the approximation factor ranged between 0.0475 and 149.82; thus, it takes some values in this range. Fig. 19 shows that it is necessary to have an approximation factor less than 1 to guarantee an adequate topology. A correct definition of the approximation factor is required to avoid the possibility of disconnected material regions. It is worth mentioning that a value of 1 was also assigned for the state variable.

With the proposed methodology, the state of each cellular automaton can change from zero to one or from one to zero, meaning that the voids can become material points and vice versa. Fig. 20 presents the results of the application of the proposed methodology. The optimal solution has no internal slots but features a curved boundary that narrows at the mid-height. This solution achieved a E/m ratio of 6.06, representing a 400% increase over the initial solution. The energy distribution is uniform within the plate. Convergence was achieved in just fourteen iterations, demonstrating the efficiency of the methods. Notably, the solution increased threefold since the second iteration.

The hysteresis cycle obtained while applying cyclic displacements to the damper is a simple graphical way to observe the advantage of applying topological optimization. Fig. 21 shows the hysteresis cycle both for the SSD damper with vertical slots and for the configuration obtained with HCA. An increase in the initial stiffness before yielding is observed. A hardening process with the increment of the displacements is also observed. Visually, it is possible to appreciate the significant change in the area of the loops. It is worth mentioning that the effect of the displacement protocol affects hysteresis, but this condition is not assessed in this research.

Table 2 presents a comparison with respect to the results obtained in [13,23]. The first research used a Bidirection evolutionary structural optimization (BESO) algorithm, while the second used the simulated annealing. These algorithms typically correspond to gradient and heuristic topology/shape optimization approaches, respectively. The first column refers to the weight of the optimal solutions. The first study maintained the weight during the optimization process. As observed, the plate obtained in this research weights 13% more. The initial Energy Dissipation Capacity (EDC) differs slightly between the three studies, possibly due to the modeling details. Such differences do not affect the conclusions of the comparison. When computing the energy-mass ratio, it is possible to compare several cases. This research presents the highest performance, including an increment of 350% from

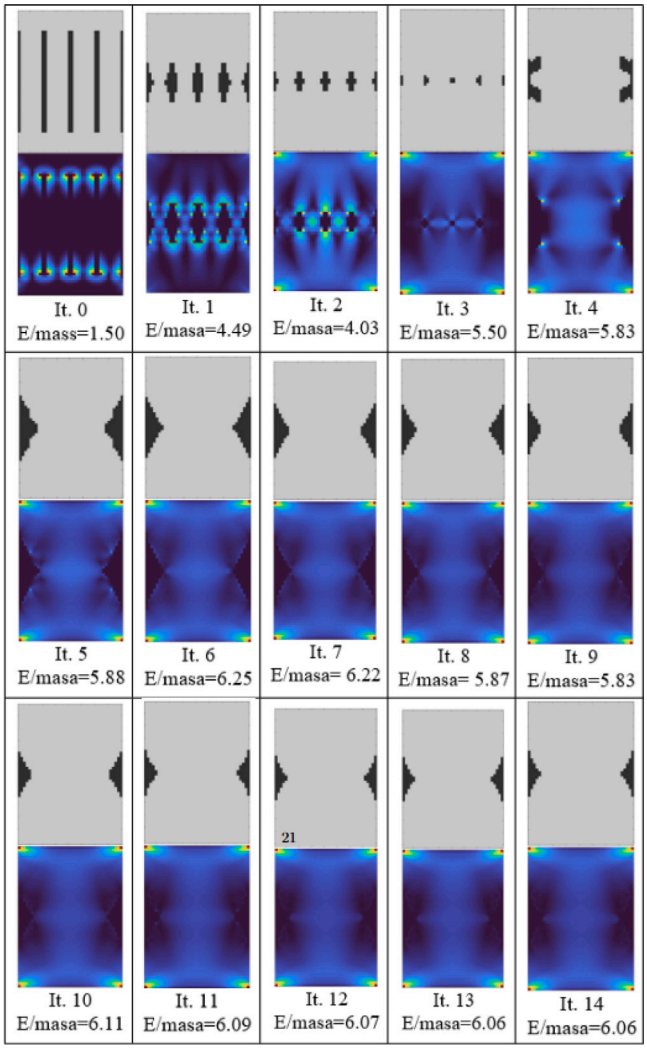

Fig. 20. Iterative process for the SSD damper with vertical slots.

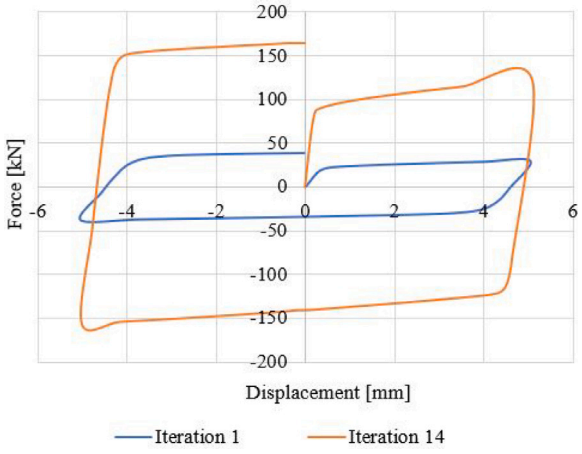

Fig. 21. Hysteresis Cycle for the initial and optimal configuration.

the initial solution. Finally, the CA-solution reduce to 32% the number of iterations compared with those required in [23] and 28% compared to values reported in [13]. Thus, the proposed methodology presents an advantage from a computational point of view.

6.2. Assessing the impact of the initial configuration in the optimal solution

One challenge found in the shape optimization of SSD dampers is defining its initial configuration. This is because there are many feasible solutions and no rules exist for choosing the most appropriate one. In addition, selecting the best from a set of possible configurations does not guarantee that the optimal solution will be obtained. Thereby, typical slot shapes such as rectangles, circles, rhombic, and squares are used (see Fig. 22). In this research, the proposed CA was applied to five additional configurations of slots: (a) one circular slot with a 25 mm radius, (b) two circular slots with 18 mm of radius, (c) four circular slots with a 12.5 mm radius, (d) four horizontal rectangular slots of 60 mm × 8 mm and (e) four square slots of 22.5 mm of side. Cases (a) to (c) are used to verify the effect of the number and size of the slots.

Figs. 23 present the results of the energy dissipation distribution for different initial configurations with rectangular slots. The maximum E/M ratio obtained is observed to be 3.82 J/kg, with the dissipation of the primary energy occurring around the edges of the slots. The lowest E/M ratio corresponds to the case of vertical slots, with a value of 1.50 J/kg. There are concentrations of energy dissipation in the corners of the slots and between slots for the initial configurations. However, the optimal solutions at the bottom present the same topology for all initial cases, with an increase in the mass of the damper and a reduction in the middle height of the damper. The obtained configurations have an average E/m ratio of 6.05 J/kg and a maximum difference of 0.05 J/kg. The energy distribution shows a remarkably high use of the vertical center region of the SSD damper, with a higher concentration on the corners of the damper. Another advantage of the algorithm is that running it multiple times for the same configuration is unnecessary, unlike stochastic heuristics.

The behavior of the algorithm, as shown in Fig. 24, is observed when analyzing an SSD damper with circular slots for different numbers of slots while maintaining the same area of voids. These circular shapes are superior to the rectangular ones, with the minimum ratio E/m being 2.90 J/kg and the maximum being 4.12 J/kg, values higher than those reported in Fig. 23. In this case, the average value is also 6.05 J/kg and a difference of 0.07 J/kg. The results proved that the algorithm can achieve the optimal solution with varying amounts and distribution of circular slots. This is in agreement with the findings of Ref. [13], where the final topology strongly depends on the initial configuration. It is recommended that further tests be conducted with different boundaries, although this is beyond the scope of current research.

6.3. Convergence process

Fig. 25 presents the results of the convergence process for the objective function related to the energy $f(U)$ and the mass $g(M)$, as well as the weighted combination. As expected, the increment in the EDC happens with the increment in the number of iterations. Concerning the mass, it would be desirable for the mass to increment, but it is observed that, in general, the mass rises slightly and linearly. Another important aspect is that fewer than fifteen iterations are needed to achieve the optimal solution in all cases. In most cases the shape achieve an E/m ratio close to 90% of the optimal value with only five iterations. This helps to control the computational cost associated with the optimization process. From the results, it is possible to conclude that the approximation for the E/m ratio is suitable to understand the problem. In practice, it will be necessary to have a target EDC for a given structure and seismic hazard. Thus, this formulation can help to assume a specific contour, as the initial slot shape is not influenced.

Table 2
Comparison with previous research.

Author	Ghabraie et al. [23]	Ferrer-Fuenmayor and Villalba-Morales [13]	This Research
Initial EDC (J)	1124	1085	1132
Final EDC	2203	4007	5119
Final Mass (gr)	747	747	844.7
Ratio final E/M	2.94	5.36	6.06
Increase (%)	96	269	350
Iterations	44	50	14

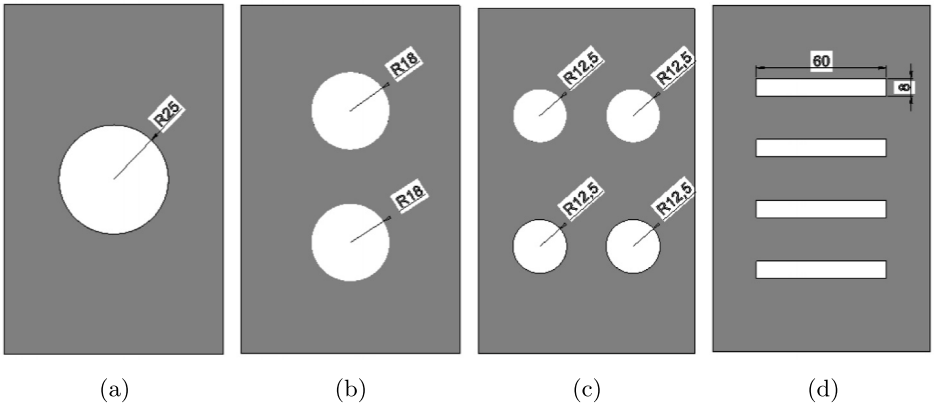

Fig. 22. Initial configurations: (a) One circular slot, (b) Two circular slots, (c) Four circular slots and (d) Four horizontal slots.

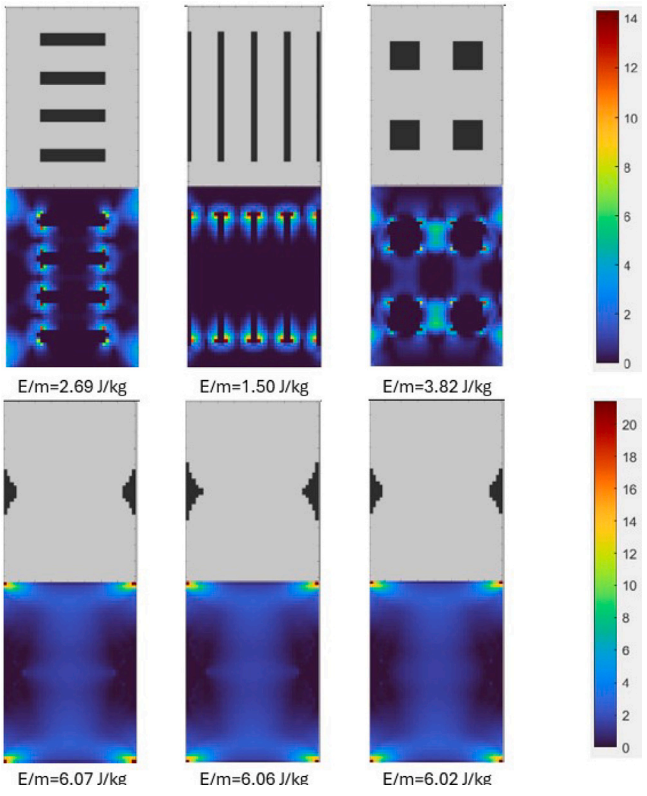

Fig. 23. Optimization process for configurations with rectangular slots.

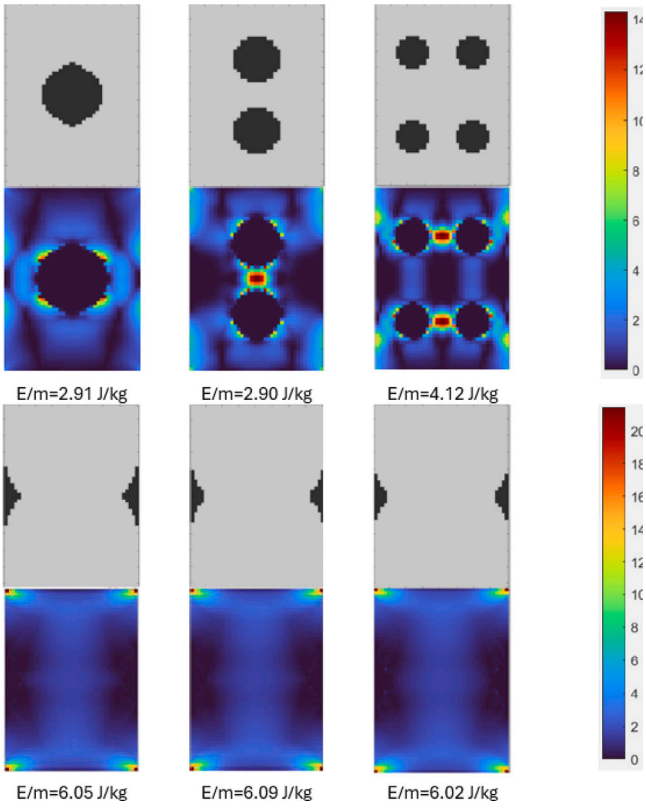

Fig. 24. Optimization process for configurations with circular slots.

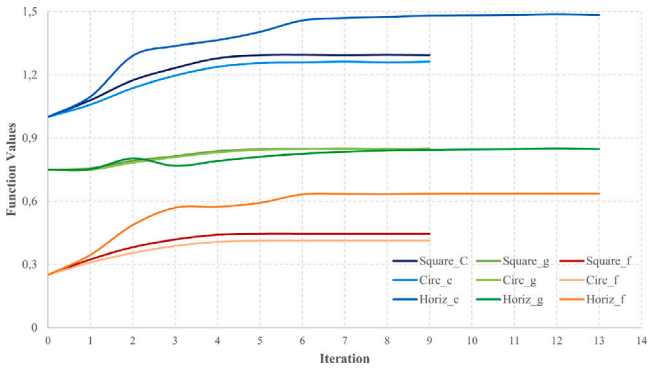

Fig. 25. Convergence process of the functions f, g and c.

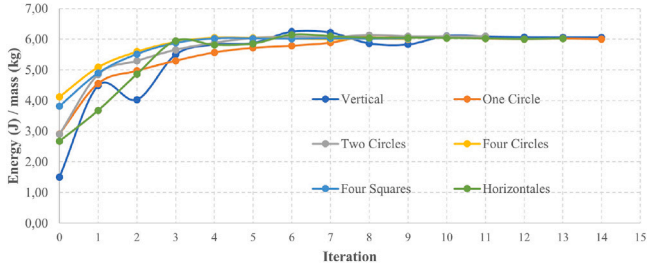

Fig. 26. Convergence process of the E/M ratio.

Using circular slots reduces the number of iterations required to achieve the solution. Some additional issues are discussed in the following section. Fig. 26 shows the convergence of the E/m ratio. The solution achieved at least 90% of the optimal value for all tested cases in a few iterations. These results reinforce the CA's ability to find the optimal solution with only a few low finite-element analysis.

6.4. Effect of load and geometrical asymmetry

Another aspect introduced into the algorithmic formulation was the imposition of a symmetric solution with respect to two orthogonal axes crossing the center of the damper. Fig. 27 presents three cases of initial non-completely symmetric conditions, along with their corresponding Von Mises stress states. Due to the symmetry of the load, when the solution is reflected across a symmetric axis, the stress states are also reflected. Not all solutions caused yielding through the entire damper. This raises the question of what would happen if symmetry were not imposed on the optimization process or the initial condition. Fig. 28 shows the result of eliminating the restriction for symmetry for the CA-based algorithm for a initial SSD configuration with an asymmetric circle slot. The results indicate that the algorithm tends to find the same optimal topology for the SSD damper presented in Fig. 20 despite the initial solution not being symmetric.

Above all, assuming that a displacement load is not symmetrical in an earthquake event, this would allow the width for the top and bottom of the device to be different. Fig. 29 presents an asymmetric protocol used to optimize the configuration of the SSD damper presented in iteration zero of Fig. 30. After the execution of the CA-based algorithm, the results have yet to be compared with the best configuration obtained in Fig. 20. Such results would indicate that the algorithm has the ability to optimize in asymmetric loads and geometric conditions.

6.5. Effect of multiple load cycles

An approximation made in this study is that the optimal solution was found considering one cycle of displacement on the device. First, it was analyzed the case where the plate presented two and four slots, as shown in Fig. 31. In this case, the sections with two and four slots supported 15 and 4 cycles, with a EDC of 32680J and 3991J, respectively. For the last cycle, both plates have yielded in most areas. In addition, the structural response of the initial and optimal shape of the damper in Fig. 15 was analyzed to be subjected to repetitive cycles. It was found that the initial shape resisted 23 cycles, producing an EDC of 19357 J, while the optimal shape supported only nine cycles with an EDC of 31841 J. Fig. 32 shows the Von Misses stresses for the plate after the loading processes. The yield was observed to propagate to the middle height of the plate in the initial configuration, indicating under-utilization of the material. In the case of the optimal solution, a better distribution of the stresses was observed. These results highlight the importance of considering multiple cycles in the optimization process and the necessity of implementing failure criteria.

6.6. Effect of height/width ratio

Finally, the definition of the initial width/height ratio is discussed. In this research, initial values were assumed to be compared with results from the literature. However, it is possible to conserve the same quantity of material for different shapes. Fig. 33 presents the stress distribution and energy dissipation capacity for different width-height $W-H$ ratios considering one rectangular slot. As expected, as the $W-H$ ratio decreases, the EDC increases, with a difference of more than 10,000 joules for the extreme cases. This is because more material is

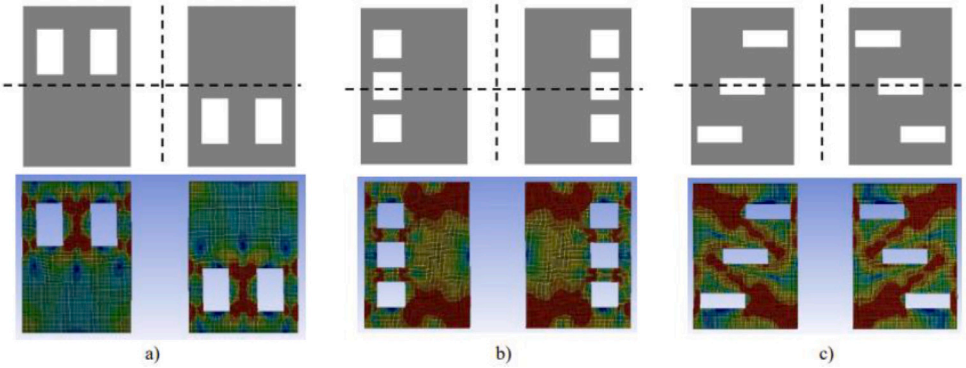

Fig. 27. Effect of non-symmetry.

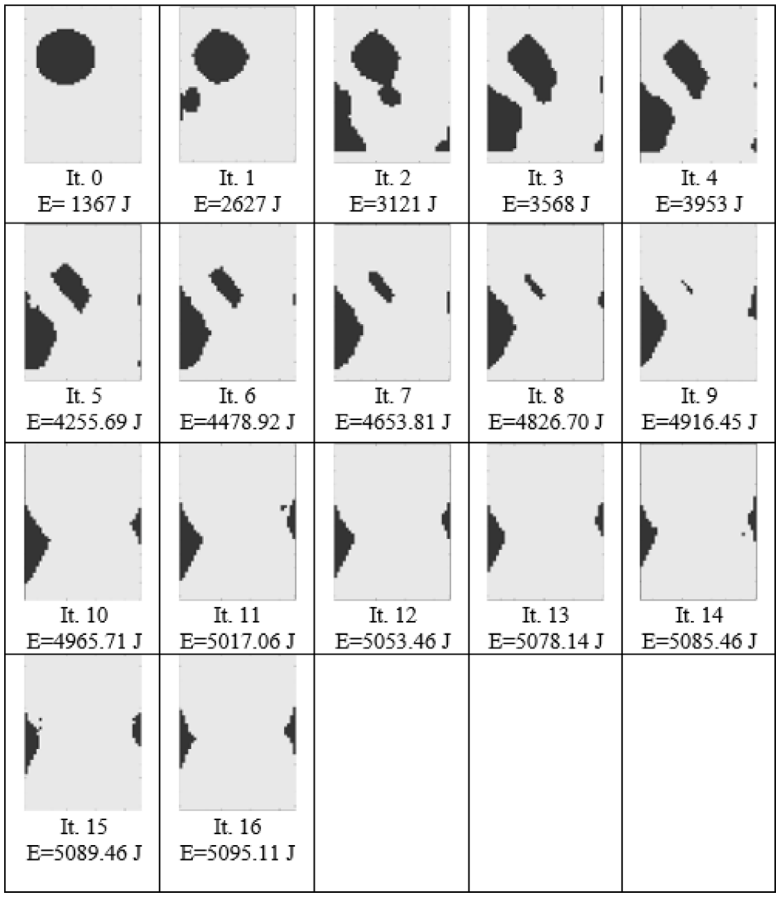

Fig. 28. Application of the CA-based algorithm for the optimization of a SSD damper with an asymmetric initial configuration.

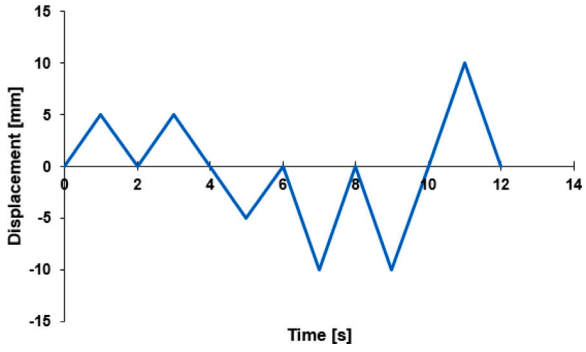

Fig. 29. Asymmetric cyclic load protocol.

directly stressed from their connection to the superior beam. However, it is necessary to consider that, as the width increases, it becomes more difficult to guarantee a total displacement restraint on the bottom side of the dampers. Such results shows the necessity of modifying the problem to determine the optimal design in a semi-opened space where a target EDC should be achieved.

7. Conclusions

This paper presented a new methodology for optimizing the shape of steel slotted dampers based on the hybrid cellular automata technique. Several examples were used to test the proposed methodologies, with the following findings:

- The CA-based algorithm found results that improve in at least 300% the energy dissipation capacity of an initial configuration tested with vertical slots.
- The computational implementation of the proposed methodology proved to be not difficult and it can be adapted to other type of steel hysteretic dampers.
- It was possible to formulate an optimization problem where the mass can vary through the optimization process, considering the quality measure as the dissipated energy/mass ratio.
- The optimal shape is less dependent on the optimal solution obtained, as it was found for most tested trajectories.
- The algorithm requires fewer than 15 iterations to get the optimal result for all the cases. This situation is a positive aspect for reducing the computational cost.

There exist some further investigations that need to be conducted. The first issue is related to the carrying out of an experimental test on several configurations of SSD dampers to obtain a better description of the low-cycle fatigue. In addition, it is necessary to understand the use

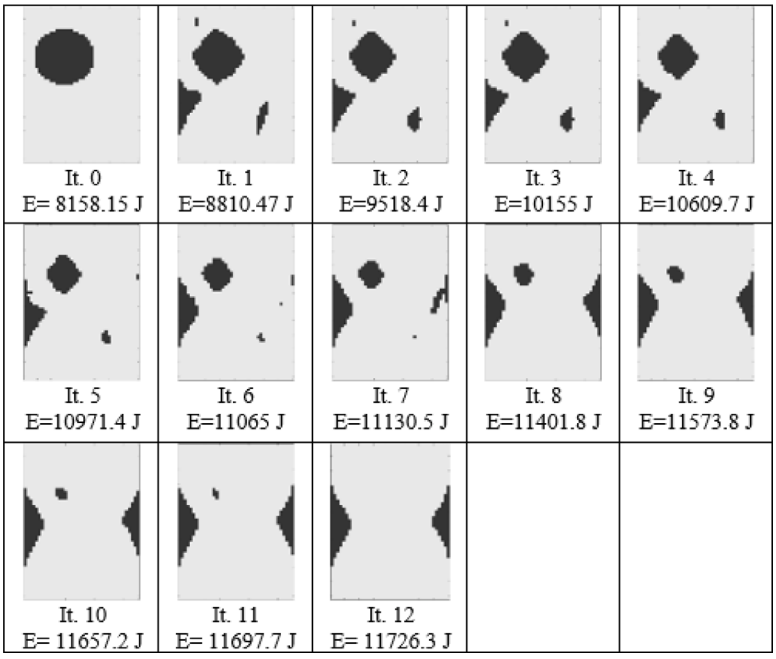

Fig. 30. Application of the CA-based algorithm for the optimization of a SSD damper with an asymmetric cyclic load displacement.

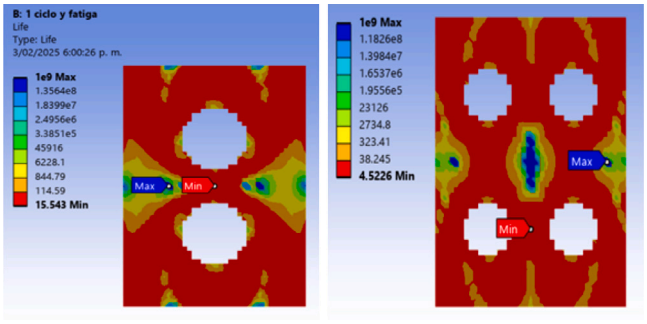

Fig. 31. Response of a SSD damper with two and four slots under several cycles of displacements.

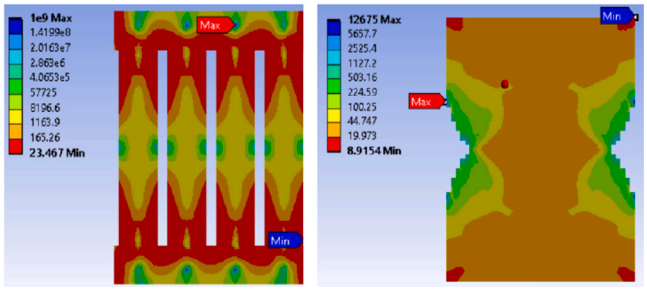

Fig. 32. Response of the initial vertical and optimal devices under several cycles of displacements.

of non-symmetrical cyclic displacement protocols to represent the real situation under an earthquake, eliminating the symmetry concerning the x-axis, and using several load displacement cycles.

CRediT authorship contribution statement

Angie Mendoza-Cuy: Writing – original draft, Visualization, Validation, Software, Methodology, Investigation, Formal analysis, Conceptualization. **Oscar Begambre-Carrillo:** Writing – original draft, Validation, Supervision, Methodology, Investigation, Conceptualization. **Jesús D. Villalba-Morales:** Writing – original draft, Visualization, Validation, Supervision, Methodology, Conceptualization.

Declaration of competing interest

The authors declare the following financial interests/personal relationships which may be considered as potential competing interests: Angie Mendoza reports financial support was provided by Industrial University of Santander. If there are other authors, they declare that they have no known competing financial interests or personal relationships that could have appeared to influence the work reported in this paper.

Acknowledgments

The first author thanks the scholarship granted to the Universidad Industrial the Santander for master students, which allowed conducting this research. In addition, Dr. Begambre and Dr. Villalba-Morales thank the universities involved for making this collaborative research possible.

Data availability

The datasets generated and/or analyzed during the current study are available from the corresponding author upon reasonable request.

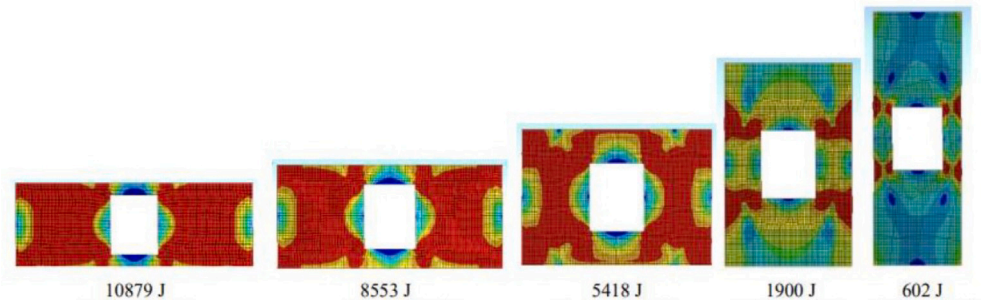

Fig. 33. Effect of Height/width ratio.

References

[1] Demertzis K, Demertzis S, Iliadis L. A selective survey review of computational intelligence applications in the primary subdomains of civil engineering specializations. Appl Sci (Switzerland) 2023;13:3380. http://dx.doi.org/10.3390/app13063380.

[2] Engelbrecht AP. Computational intelligence: An introduction. 1st ed. West Sussex, London: John Wiley & Sons, Ltd; 2007.

[3] Sumathi S, Pannerselvam S. Computational intelligence paradigms: Theory & applications using MATLAB. 1st ed. New York: CRC Press; 2019.

[4] Wolfran S. Statistical mechanics of cellular automata. Rev Modern Phys 1983;55:601–44.

[5] Vaidyanathan CV, Kamatchi P, Ravichandran R. Artificial neural networks for predicting the response of structural systems with viscoelastic dampers. Comput-Aided Civ Infrastruct Eng 2005;20:294–302.

[6] Abdulateef WS, Hejazi F. Fuzzy logic based adaptive vibration control system for structures subjected to seismic and wind loads. Structures 2023;55:1507–31. http://dx.doi.org/10.1016/j.istruc.2023.06.108.

[7] Miguel LFF, Miguel LFF, Lopez RH. Methodology for the simultaneous optimization of location and parameters of friction dampers in the frequency domain. Eng Optim 2018;50:2108–22. http://dx.doi.org/10.1080/0305215X.2018.1428318.

[8] Cetin H, Aydin E, Ozturk B. Optimal design and distribution of viscous dampers for shear building structures under seismic excitations. Front Built Environ 2019;5:90. http://dx.doi.org/10.3389/fbuil.2019.00090.

[9] Tu X, He Z, Huang G. Performance-based multi-objective collaborative optimization of steel frames with fuse-oriented buckling-restrained braces. Struct Multidiscip Optim 2020;61:365–79. http://dx.doi.org/10.1007/s00158-019-02366-9.

[10] Djerouni S, Ounis A, Elias S, Abdeddaim M, Rupakhety R. Optimization and performance assessment of tuned mass damper inerter systems for control of buildings subjected to pulse-like ground motions. Structures 2022;38:139–56. http://dx.doi.org/10.1016/j.istruc.2022.02.007.

[11] Aminzadeh M, Kazemi HS, Tavakkoli SM. A numerical study on optimum shape of steel slit dampers. Adv Struct Eng 2020;23:2967–81. http://dx.doi.org/10.1177/1369433220927281.

[12] Kim YC, Mortazavi SJ, Farzampour A, Hu JW, Mansouri I, Awoyera PO. Optimization of the curved metal damper to improve structural energy dissipation capacity. Buildings 2022;12:67. http://dx.doi.org/10.3390/buildings12010067.

[13] Ferrer-Fuenmayor S, Villalba-Morales JD. Shape optimization of slotted steel plate dampers using the simulated annealing algorithm. J Appl Comput Mech 2023;9:870–83. http://dx.doi.org/10.22055/jacm.2023.42249.3895.

[14] Qiao G, Hong Y, Ou J. Quantitative monitoring of pitting corrosion based on 3-D cellular automata and real-time ENA for RC structures. Measurement: J Int Meas Confed 2014;53:270–6. http://dx.doi.org/10.1016/j.measurement.2014.03.045.

[15] Schadschneider A. Cellular automata models of highway traffic. Phys A 2006;372:142–50. http://dx.doi.org/10.1016/j.physa.2006.05.011.

[16] Su H, Wen Z, Qian C. Cellular automata-based analysis for seepage failure process of earth-rock dam. Struct Control Heal Monit 2020;27:e2553. http://dx.doi.org/10.1002/stc.2553.

[17] de S. M. Ozelim LC, Cavalcante ALB. 3D cellular automata as a computational tool to generate artificial porous media. Int J Geomech 2018;18. http://dx.doi.org/10.1061/(asce)gm.1943-5622.0001242.

[18] Feng C, Zhang N, Habiyakare T, Yu H. Development of a cellular automata-based distributed hydrological model for simulating urban surface runoff. J Hydrol 2023;627:130348. http://dx.doi.org/10.1016/j.jhydrol.2023.130348.

[19] Araghi SK, Stouffs R. Exploring cellular automata for high density residential building form generation. Autom Constr 2015;49:152–62. http://dx.doi.org/10.1016/j.autcon.2014.10.007.

[20] Tovar A. Optimización topológica con la técnica de los autómatas celulares híbridos. Rev Int Mét Num Cálc Dis Ing 2005;21:365–83.

[21] Grubits P, Cucuzza R, Habashneh M, Domaneschi M, Aela P, Rad MM. Structural topology optimization for plastic-limit behavior of I-beams, considering various beam-column connections. Mech Based Des Struct Mach 2024. http://dx.doi.org/10.1080/15397734.2024.2412757.

[22] Habashneh M, Cucuzza R, Domaneschi M, Rad MM. Advanced elasto-plastic topology optimization of steel beams under elevated temperatures. Adv Eng Softw 2024;190:103596. http://dx.doi.org/10.1016/j.advengsoft.2024.103596.

[23] Ghabraie K, Chan R, Huang X, Xie YM. Shape optimization of metallic yielding devices for passive mitigation of seismic energy. Eng Struct 2010;32:2258–67. http://dx.doi.org/10.1016/j.engstruct.2010.03.028.

[24] Javanmardi A, Ibrahim Z, Ghaedi K, Ghadim HB, Hanif MU. State-of-the-art review of metallic dampers: Testing, development and implementation. Arch Comput Methods Eng 2020;27:455–78. http://dx.doi.org/10.1007/s11831-019-09329-9.

[25] Lin H, Xu A, Misra A, Zhao R. An ANSYS APDL code for topology optimization of structures with multi-constraints using the BESO method with dynamic evolution rate (DER-BESO). Struct Multidiscip Optim 2020;62:2229–54. http://dx.doi.org/10.1007/s00158-020-02588-2.

[26] He H, Wang X, Zhang X. Energy-dissipation performance of combined low yield point steel plate damper based on topology optimization and its application in structural control. Adv Mater Sci Eng 2016;5654619. http://dx.doi.org/10.1155/2016/5654619.

[27] Briones B, de la Llera JC. Analysis, design and testing of an hourglass-shaped copper energy dissipation device. Eng Struct 2014;79:309–21. http://dx.doi.org/10.1016/j.engstruct.2014.07.006.

[28] Zhang C, Wang L, Sun C, Wu M. Feasibility of the evaluation of the deformation capacity of the shear panel damper by FEM. J Constr Steel Res 2018;147:433–43. http://dx.doi.org/10.1016/j.jcsr.2018.04.033.

[29] Xu LY, Nie X, Fan JS. Cyclic behaviour of low-yield-point steel shear panel dampers. Eng Struct 2016;126:391–404. http://dx.doi.org/10.1016/j.engstruct.2016.08.002.

[30] Mari GD, Domaneschi M, Ismail M, Martinelli L, Rodellar J. Reduced-order coupled bidirectional modeling of the Roll-N-Cage isolator with application to the updated bridge benchmark. Acta Mech 2015;226:3533–53. http://dx.doi.org/10.1007/s00707-015-1394-3.

[31] Domaneschi M. Simulation of controlled hysteresis by the semi-active Bouc-Wen model. Comput Struct 2012;106–107:245–57. http://dx.doi.org/10.1016/j.compstruc.2012.05.008.

[32] Khatibinia M, Jalaipour M, Gharehbaghi S. Shape optimization of U-shaped steel dampers subjected to cyclic loading using an efficient hybrid approach. Eng Struct 2019;197:108874. http://dx.doi.org/10.1016/j.engstruct.2019.02.005.

[33] of Civil Engineers AS. ASCE STANDARD ASCE/SEI 7-16 minimum design loads and associated criteria for buildings and other structures. ANSI/ASCE Stand 2016;1–330.

[34] Applied Technology Council. FEMA 461- interim testing protocols for determining the seismic performance characteristics of structural and nonstructural components. Washington: Federal Emergency Management Agency; 2007, www.ATCouncil.org.

[35] Aisc. Seismic Provisions for Structural Steel Buildings Supersedes the Seismic Provisions for Structural Steel Buildings, dated July 12, 2016, and all previous versions Approved by the Committee on Specifications. 2022.

[36] CEN. EN-151292 Anti-seismic Devices. Brussels: European Committee for Standardization; 2019.

[37] Ministry of Construction of the People's Republic of China (MCPRC). Dampers for vibration energy dissipation of buildings (JG/T 209–2012). Beijing: China Construction Industry Press; 2012.

[38] Building Center of Japan. Specifications for BRB certification. Tokyo: The building Center of Japan; 2017.

[39] Deng K, Pan P, Sun J, Liu J, Xue Y. Shape optimization design of steel shear panel dampers. J Constr Steel Res 2014;99:187–93. http://dx.doi.org/10.1016/j.jcsr.2014.03.001.

[40] Zhu B, Wang T, Zhang L. Quasi-static test of assembled steel shear panel dampers with optimized shapes. Eng Struct 2018;172:346–57. http://dx.doi.org/10.1016/j.engstruct.2018.06.004.

[41] Liu Y, Shimoda M. Shape optimization of shear panel damper for improving the deformation ability under cyclic loading. Struct Multidiscip Optim 2013;48:427–35. http://dx.doi.org/10.1007/s00158-013-0909-6.

[42] Farzampour A, Khatibinia M, Mansouri I. Shape optimization of butterfly-shaped shear links using Grey Wolf Algorithm. Int J Earthq Eng-Ing Sismica 2019;36:1–15.
[43] Pfeifer B, Kugler K, Tejada MM, Baumgartner C, Seger M, Osl M, Netzer M, Handler M, Dander A, Wurz M, Graber A, Tilg B. A cellular automaton framework for infectious disease spread simulation. Open Med Informatics J 2008;2:70–81.
[44] Xie J, Zhang L. Application of cellular automata with improved dynamic analysis in evacuation management of sports events. J Sensors 2022;2022:878865. http://dx.doi.org/10.1155/2022/8782865.
[45] Shen L. Simulation of employee behaviour psychology based on stochastic cellular automata. Curr Psychol 2024;43:6770–82. http://dx.doi.org/10.1007/s12144-023-04823-7.
[46] Burraston D, Edmonds E. Cellular automata in generative electronic music and sonic art: A historical and technical review. Digit Creativity 2005;16:165–85. http://dx.doi.org/10.1080/14626260500370882.
[47] Chen T, Lin J. A novel model for the evolution of online public opinion based on fuzzy cellular automata rules in directed world networks. Appl Math Inf Sci 2013;7:2335–43. http://dx.doi.org/10.12785/amis/070625.
[48] Su S, Ju X. A cellular learning automata-based approach for self-protection and coverage problem in the Internet of Things. Internet Things (Netherlands) 22:100718. http://dx.doi.org/10.1016/j.iot.2023.100718.
[49] Li X, Wu J, Li X. Theory of practical cellular automaton. Beijing: Springer; 2018.
[50] Hadeler K-P, Müller J. Cellular automata: Analysis and applications. Cham, Switzerland: Springer; 2017.